Instrumentation for the Breath-by-Breath Determination of Oxygen and Carbon Dioxide Based on Nondispersive Absorption Measurements

Peter B. Arnoudse[1] and Harry L. Pardue*

Department of Chemistry, Purdue University, West Lafayette, Indiana 47907-1393

Joe D. Bourland, Robert Miller,[2] and Leslie A. Geddes*

Hillenbrand Biomedical Engineering Center, Purdue University, West Lafayette, Indiana 47907

This paper describes the development and evaluation of instrumentation for the breath-by-breath determination of oxygen and carbon dioxide in respiratory gases. The method is based on nondispersive absorption and uses the 145-nm absorption band for detection of oxygen and the 4.3-μm band for detection of carbon dioxide. A xenon discharge lamp with a sharp band at 147 nm was chosen as the source for the determination of oxygen, and a carbon dioxide discharge lamp with a sharp band at 4.3 μm was chosen for determination of carbon dioxide. A vacuum photodiode was used as the detector for oxygen, and a photoconductive cell with a built-in interference filter was used for detection of carbon dioxide. Plots of absorbance (A) vs concentration (C, %) were linear for oxygen and were nonlinear for carbon dioxide. Typical least-squares calibration equations were $A = 0.020C + 0.02$ for oxygen (0–100%) and $A = 0.0012C^2 + 0.050C + 0.008$ for carbon dioxide (0–8%). Comparisons of computed (y) vs prepared (x) values for the concentrations given above were linear for both gases, yielding $y = (1.00 \pm 0.01)x - 0.13 \pm 0.73$ for oxygen and $y = (1.07 \pm 0.02)x - 0.04 \pm 0.06$ for carbon dioxide. The standard deviations were 1.2% at 50% oxygen and 1.5% at 4% carbon dioxide. Records are presented to illustrate breath-by-breath monitoring of these gases in a healthy subject.

INTRODUCTION

Breath-by-breath monitoring of oxygen and carbon dioxide concentrations in inspired and expired air are important in a variety of physiological and clinical studies (*1*, *2*). For example, the expired oxygen concentration can change very quickly during anaesthesia in patients subject to malignant hyperthermia, a condition that is fatal if not diagnosed and treated immediately (*3*). Many of the methods for detecting respiratory gases have been reviewed elsewhere (*4–6*); however, none of these methods satisfies all the criteria for rapid respiratory monitoring, namely rapidity of response, noninvasiveness, manageability, and economy (*7*). For oxygen, the methods in most common use are based on electrochemical, paramagnetic, and mass spectrometric measurements. For carbon dioxide, the most common methods are nondispersive infrared (IR) photometry and mass spectrometry. Mass spectrometry and nondispersive infrared photometry (for carbon dioxide) are the most practical. However, no methods in current use are completely satisfactory, as evidenced by recent papers describing a Raman spectroscopic approach for oxygen and carbon dioxide as well as selected anaesthetic gases (*8*).

The present study was undertaken to develop and evaluate optical absorption methods for breath-by-breath determination of oxygen and carbon dioxide. It was expected that optical methods would have the short response time necessary for breath-to-breath determinations, be noninvasive, be compact enough to stand alone, and be interfaced easily with existing monitoring equipment, as well as be sufficiently economical in terms of both capital and operational costs to be practical clinically.

Vacuum ultraviolet (VUV) absorption was used for detection of oxygen, and infrared absorption, for detection of carbon dioxide. Oxygen has a strong absorption band at 145 nm where the absorption by other respiratory gases in negligible (*9–12*). Although earlier studies (*13*, *14*) demonstrated the general feasibility of this approach, a more extensive study (*14*) resulted in a method suitable over a very narrow concentration range (11–20%). Carbon dioxide has an absorption band at 4.3 μm. Current applications of this band involve broad-band sources, mechanical choppers, and optical filters. In this study we used electrically-pulsed gas-discharge lamps and ac detection circuitry. The band at 4.3 μm from a carbon dioxide discharge lamp (*15*) was used for detection of carbon dioxide, and the line at 147 nm from a xenon discharge lamp was used for detection of oxygen.

EXPERIMENTAL SECTION

The experimental approach combined two important goals: (1) design of the simplest possible instrumentation and (2) maximization of the overlap among instrumental components for the two gases.

Instrumentation. Figure 1 is a conceptual representation of the instrument. Respiratory gases are drawn through the region between the radiators and detectors. The radiation from the sources, S_1 and S_2, passes through the respiratory gases in the sample tube, and transmitted radiation is sensed by the detectors, D_1 and D_2. The signals from these detectors are amplified by suitable circuitry. The shorter path length is for oxygen and reflects the fact that its absorptivity is much higher than that for carbon dioxide.

Radiation Sources. Gas-discharge lamps with external electrodes were used in both cases to generate radiant energy. Initial studies with gas-discharge lamps designed and built in our laboratories led to custom-built lamps (Opthos Instruments, Inc., Rockville, MD); details of the lamps built in our laboratory appear elsewhere (*6*). The commercial discharge lamps for oxygen (S2) and carbon dioxide (S1) were the same except for the filling gases. The xenon discharge lamp used for oxygen included an evaporated getter that maintained the purity of the gas inside the lamp. Both lamps had magnesium fluoride windows and either were enclosed in aluminum boxes with holes for the lamps to protrude or were surrounded by grounded wire mesh (70% open space) to prevent radiation of the radiofrequency (rf) power used to excite the lamps.

The filling procedures for the discharge lamps were adapted from an earlier report (*18*). Complete details, including a schematic diagram of the gas-handling system are described elsewhere (*6*), and the procedure is discussed only briefly here. The lamp envelopes were first cleaned by immersion in a 1:1 mixture of

[1] Dow Chemical Co., Freeport, TX 77541.
[2] Colorado State University, Fort Collins, CO 80523.

0003-2700/92/0364-0200$03.00/0

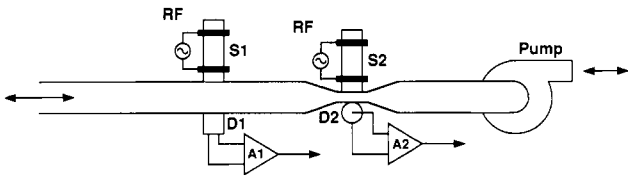

Figure 1. Schematic representation of instrumentation for breath-by-breath determination of oxygen and carbon dioxide: (S_1, S_2) radiant-energy sources for carbon dioxide and oxygen; (D_1, D_2) detectors for carbon dioxide and oxygen; (A) amplifiers; (RF) radio-frequency sources.

concentrated sulfuric acid and nitric acid for several minutes, after which they were rinsed thoroughly with distilled water and permitted to dry in air. Then they were cycled three times using evacuation to 10^{-5} Torr, filling to about 1-Torr pressure with the desired gas, and then reevacuation to about 10^{-5} Torr with rf power applied. After the third cycle, the lamps were filled to the desired pressure with the appropriate gas and sealed.

Excitation of Discharge Lamps. The lamps were excited by external electrodes to which high-voltage, pulsed rf was applied from a resonant circuit consisting of a coil and capacitor tuned to resonate at a frequency of 27 MHz. A 500-Hz square-wave generator (Model EU-81A Function Generator, Health Co., Benton Harbor, MI) pulsed the 27-MHz sine-wave rf generator. The pulsed 27-MHz rf was amplified by a 10-W-amplifier (Model 310L rf power amplifier, ENI, Rochester, NY) and fed to the coil by a coaxial cable connected between two turns from one end of the coil. The ends of the coil were connected to ribbon electrodes wrapped around the ends of the discharge tube.

Sample Cells. The sample cell for carbon dioxide consisted of a segment of square quartz tubing with 1-mm wall thickness and 3-mm inner dimensions (Wilmad Glass Co., Inc., Bueua, NJ). The transmittance of the cell was approximately 30% at 4.3 μm. Commercially available windows (Wilmad Glass Co., Inc.) were used for oxygen measurement and consisted of calcium fluoride or barium fluoride, separated by Teflon washers. The path length through this cell could be varied between 0.015 and 1.0 mm by selecting the number of Teflon spacers inserted.

To prevent moisture from collecting inside the sample cells, they were heated to 40 °C, which is higher than the temperature of the respiratory gases. This was accomplished by mounting the cells on a brass plate into which $^1/_4$-W-resistors and a temperature sensor were embedded. A regulating circuit (*6*) was used to control the temperature.

Detectors. For detection of oxygen, we used a photodiode (R1187, Hamamatsu Corp., Middlesex, NJ), with a cesium iodide-surfaced photocathode, a magnesium fluoride window; it was operated at 9 V. For detection of carbon dioxide, we used a photoconductive detector (Model 505, Infrared Industries, Orlando, FL) with an interference filter having a transmission peak centered at 4.26 nm.

Detection Circuitry. The amplitude-modulated signals from the two detectors were of the same order of magnitude and allowed use of the same amplifying circuitry. Operational amplifiers were used for current-to-voltage conversion and were followed by rectification and filtering circuits (*6*). The resulting direct-current voltage had a transfer function of 1×10^8 V/A relative to the input. The resulting signal was displayed on a strip-chart recorder or a digital voltmeter, and absorbances were calculated manually.

Gas Samples. The gases studied were oxygen, carbon dioxide, water vapor, nitrous oxide, and halothane. Mixtures were prepared from commercial-grade gases in cylinders by diluting the pure gases with nitrogen. Flow meters were used to control the relative amounts of the different gases. After the gases passed through the flow meters, they were combined in a Y-tube that was connected to the inlet ports of the sample cells. In most cases, the total flow rate was 2 L/min. Solenoid valves between the gas cylinders and the flow system were used to switch rapidly from the gas mixtures to pure nitrogen which was used as the reference for 100% T measurements.

To measure the absorbance of water vapor, a stream of dry nitrogen was humidified and its transmittance was measured relative to dry nitrogen. To humidify the nitrogen, the gas was passed through a sealed tank containing water. The vapor pressure in the tank was selected by adjusting the temperature of the water therein. A hygrometer (Model 91 Dew Point Hygrometer, Yellow Springs Instrument Co., Inc., Yellow Springs, OH) was used to measure the water content of the gas stream as it exited the tank just prior to being sampled as just described.

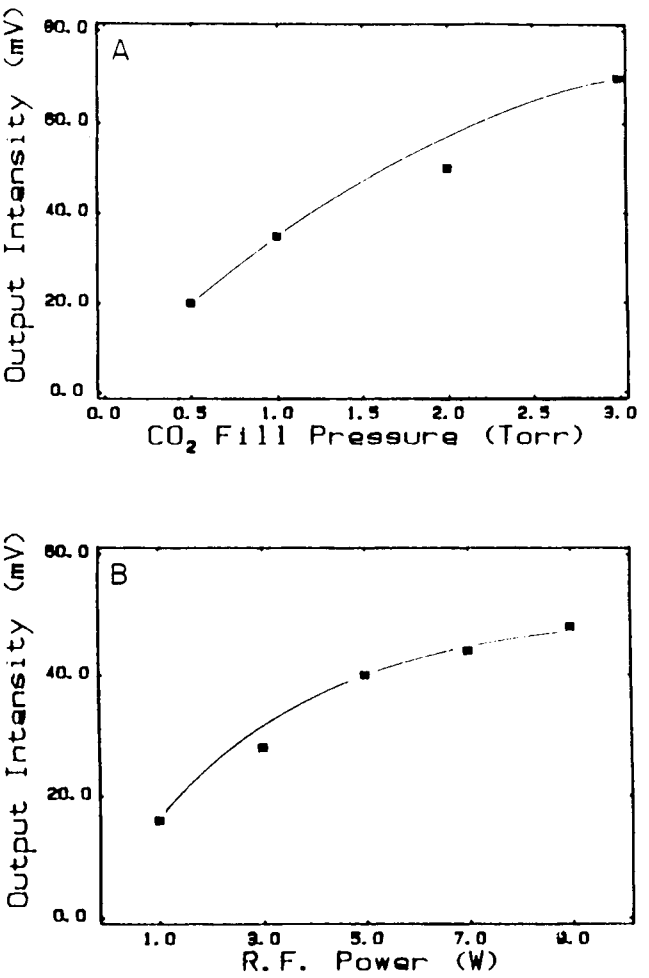

Figure 2. Output intensity versus gas pressure (A) and output intensity versus rf power (B) for the carbon dioxide discharge lamp.

An anaesthesia machine was used to deliver halothane in oxygen. The absorbance of halothane was determined by preparing mixtures of halothane and oxygen and then measuring the transmittances relative to pure nitrogen. Because oxygen, like nitrogen, is transparent in the IR region, the presence of oxygen did not cause any problem with measurements in this region. However, for VUV measurements, the absorbance due to oxygen was calculated by using the absorptivity and partial pressure and the absorbance due to halothane was computed by difference.

RESULTS AND DISCUSSION

Carbon Dioxide. The carbon dioxide lamp emitted a strong, broad band centered at 4.3 μm. The weaker band at 2.7 μm reported by others (*16–18*) was not observed. Figure 2 shows the effect of gas pressure and rf power and the output intensity measured with the detection circuitry described above. In each case, intensity increased nonlinearly with the independent variable. A gas pressure of 2 Torr was selected because a more stable discharge was maintained more easily with lower power levels. The power level used to drive the source was 8 W (maximum).

Figure 3 shows the calibration plot for carbon dioxide which curves toward the concentration axis and is best fit with a nonlinear model. The first two rows of data in Table I represent least-squares coefficients for a quadratic fit to calibration data on two different days. Agreement between the two data sets is very good. The calibration equation for the first day was used to compute concentrations from absorbance

Table I. Least-Squares Statistics of Calibration Data

	coefficients[a]				
	quadratic ± sd	linear ± sd	intercept ± sd	std error of estimate	r^2
		carbon dioxide			
day 1	−0.0012 ± 0.0002	0.050 ± 0.002	0.008 ± 0.005	0.003	0.999
day 2	−0.0013 ± 0.0001	0.049 ± 0.001	0.007 ± 0.003	0.004	0.999
		oxygen			
day 1a		0.0202 ± 0.0005	0.003 ± 0.04	0.035	0.997
day 1b		0.0200 ± 0.0004	0.02 ± 0.03	0.028	0.998
day 2		0.0206 ± 0.0006	0.005 ± 0.04	0.039	0.997
combined		0.0202 ± 0.0002	0.008 ± 0.01	0.029	0.997

[a] $A = aC^2 + bC + c$ for carbon dioxide and $A = aC + b$ for oxygen.

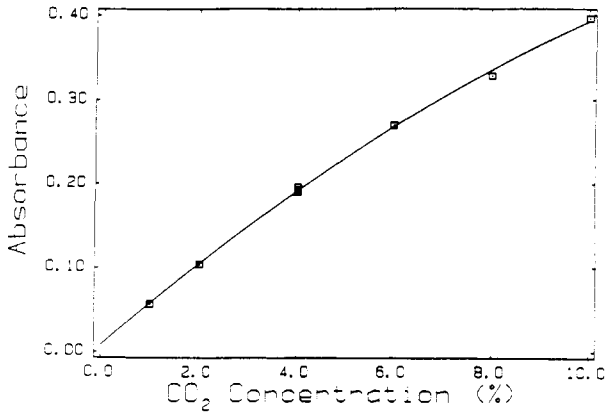

Figure 3. Calibration plot for carbon dioxide.

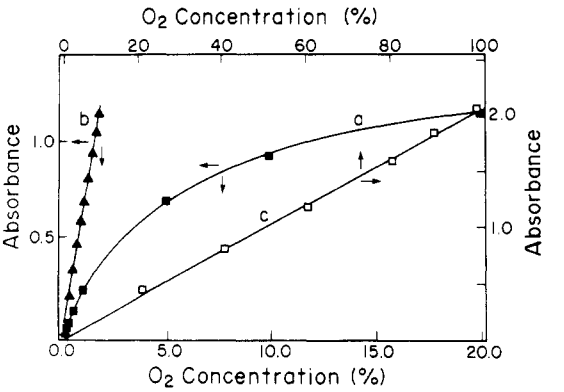

Figure 4. Calibration plots for oxygen: (a) windowless cell, oxygen discharge lamp; (b) windowless cell, xenon discharge lamp (147-nm line); (c) variable path length cell, xenon discharge lamp.

data obtained on the second day. A plot of computed versus prepared concentration was linear with a slope and intercept of +1.07 ± 0.02 and −0.04 ± 0.06, respectively.

The standard deviation of three replicates at 4% carbon dioxide concentration was 0.0030 absorbance units compared to a signal valve of 0.20. This corresponds to a relative standard deviation of 1.5%. Also, combined with the sensitivity (slope) of the calibration plot at 4% carbon dioxide (0.0383), the standard deviation of 0.0030 corresponds to a resolution of 0.08% carbon dioxide.

Oxygen. Initial experiments with oxygen were done with a windoless cell and a discharge lamp containing oxygen. Because of the large amount of unabsorbed broad-band radiation from the oxygen-filled lamp, calibration plots were nonlinear even at low concentrations of oxygen (curve a in Figure 4). When the 147-nm line from a lamp filled to 0.1 Torr with xenon and operated 8 W was used, the calibration plot became linear at low concentrations, but the sensitivity was so high (curve b in Figure 4) that deviations from linearity occurred for oxygen concentrations below 10%. To avoid this problem, we tested a shorter path length cell that consisted of two transparent windows separated by Teflon washers that could be used to vary the path length. In choosing the window material, we ruled out magnesium fluoride because the short wavelength cutoff (110 nm) would permit radiation well below 147 nm to pass and therefore cause problems at higher oxygen concentrations. Both barium and calcium fluoride have short-wavelength cutoffs closer to the desired wavelength, and these were evaluated. We chose calcium fluoride because it is less susceptible to water vapor and appeared to be more shock resistant than barium fluoride.

The photodiode used for UV detection had a dark current of about 10^{-12} A and a maximum output current of 10^{-7} A. We chose to operate in the range 10^{-8} to 10^{-11} A for oxygen concentrations between 1 and 100% to avoid overdriving the phototube at low oxygen concentrations and to have a signal level about 10-fold the dark current at the highest oxygen concentration. The use of a low current also prolongs the life of the photodiode.

It was found that a sample cell path length of 0.02 cm satisfied the foregoing criteria. For the resulting configuration that included the xenon lamp, a 0.02-cm path length sample cell with calcium fluoride windows and a vacuum photodiode, the calibration plots were linear between 0 and 100% oxygen.

The last four rows in Table I show linear least-squares fits for absorbance versus concentration for calibration data obtained on the same and subsequent days. Agreement is very good among the different data sets. When calibration data from one data set were used to compute concentrations from another data set, a least-squares fit of computed vs prepared concentrations yielded a slope and intercept of +1.00 ± 0.01 and −0.13 ± 0.73% O_2, respectively. The standard deviation for three replicates at 50% oxygen was 0.006 35 absorbance units. Dividing this by the average slope (0.0203) for the three data sets in Table I yields a resolution of 0.62% oxygen, or about 1.2% of the concentration value.

Interferences. The potential interferents studied were water vapor, nitrous oxide, and halothane.

None of these gas mixtures (water vapor, nitrous oxide, and halothane in oxygen) produced a detectable change in absorbances at the wavelength used to measure carbon dioxide. Although nitrous oxide has an absorption band at 4.5 μm, apparently the bandwidth of the interference filter used to detect carbon dioxide is sufficiently narrow to avoid significant interference.

The interference for detection of oxygen was more complex because each of the other gases, including carbon dioxide, absorb some energy in the VUV region. We evaluated absorbances of these gases using the oxygen detector. Absorptivities (cm^{-1} atm^{-1}) for carbon dioxide, water vapor, nitrous oxide, and halothane were 16.5 ± 0.5, 28.4 ± 2.6, 108 ± 4, and 487 ± 105, relative to literature values (*19*, *20*) of 17.4, 18.1, 115, and 436, respectively. Our value for water vapor is sig-

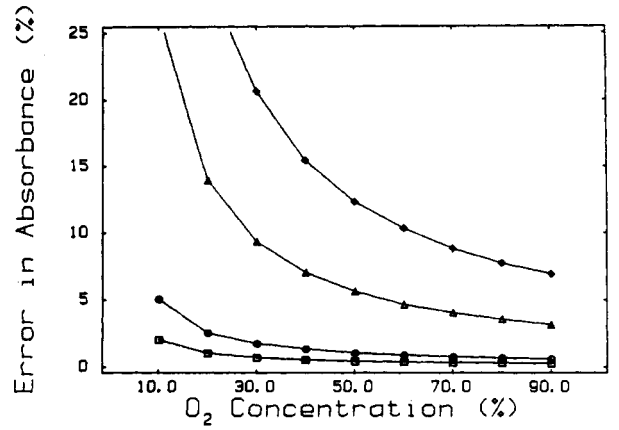

Figure 5. Computed errors for different concentrations of oxygen in the presence of different gases: (□) 4.2% carbon dioxide; (○) 6.2% water vapor; (△) 2% halothane; (♦) 20% nitrous oxide.

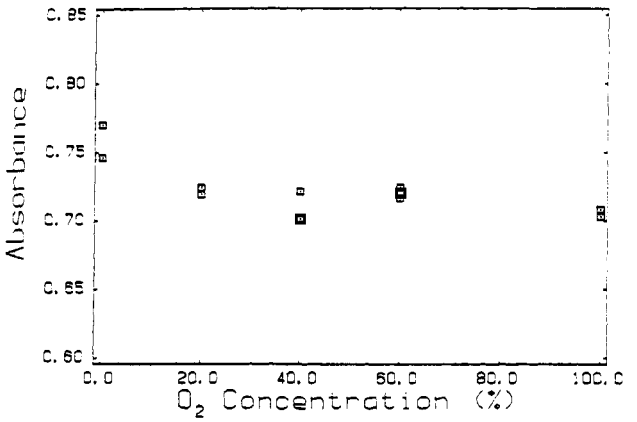

Figure 6. Effects of different concentrations of oxygen and nitrogen on absorbence of carbon dioxide (5%).

nificantly higher than the literature value, and the large uncertainty associated with the value for halothane probably results from the fact that it was determined by taking the difference between total absorbance and the absorbance due to oxygen. Our value for the absorptivity of oxygen, 350 ± 14 (n = 17) cm^{-1} atm^{-1}, is in good agreement with the literature value of 353 cm^{-1} atm^{-1} (*19*, *21*).

These absorptivities were used to compute interference of fixed concentrations of these gases in different concentrations of oxygen; the results are shown in Figure 5. Except for the lowest oxygen concentration, interferences due to expected amounts of carbon dioxide and water vapor are relatively small. However, the interferences due to halothane and nitrous oxide are significant at all oxygen concentrations, and corrections will be required by using known values of absorptivities and concentrations determined by independent methods.

We also evaluated the effect of pressure-broadening on carbon dioxide by measuring the absorbance of a 5% sample of carbon dioxide in mixtures of nitrogen and oxygen ranging from 1 to 100%. Figure 6 shows the results from two sets of experiments. After an initial drop between 100 and 80% nitrogen, the absorbance remains essentially constant for all other compositions. We do not understand the reason for the initial drop; however it is not relevant to the determination of carbon dioxide in respired gases because the situation would not be encountered.

Breath-by-Breath Measurements. The completed instrument, which included a sensor for measuring respired volume, was used (*3*) to monitor breath-by-breath concentrations of oxygen and carbon dioxide in a human subject breathing room air. A typical record is shown in Figure 7. In each case peaks and valleys are well resolved.

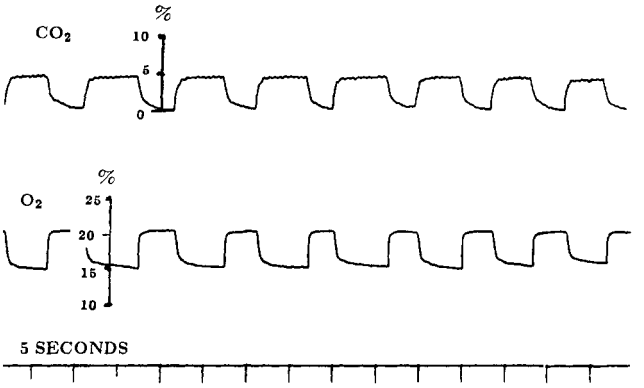

Figure 7. Carbon dioxide and oxygen concentrations recorded from the airway of a healthy subject.

As a further test of the concept, a second-generation instrument was used to monitor breath-by-breath concentrations and volumes of oxygen and carbon dioxide in pigs bred to be susceptible to malignant hyperthermia, a condition that is accompanied by a sharp increase in the consumption of oxygen and the production of carbon as a result of the increased metabolic rate that produces the increased temperature. Administration of halothane caused a very rapid increase in the uptake of oxygen (578–1490 mL/min) and production of carbon dioxide (142–622 mL/min). The increase in body temperature was much slower, increasing from 42.6 to 44.3 °C during a 5-min period. These results confirm the potential ultility of the nondispersive optical system for detecting metabolic changes that can occur under a variety of circumstances.

Conclusions. The nondispersive optical system described herein is capable of quantifying oxygen and carbon dioxide with sufficient speed and accuracy to detect breath-by-breath changes in these gases. The optimal system for oxygen detection consists of a xenon discharge lamp, a short path length sample cell with calcium fluoride windows and a vacuum phototube. The optimum system for carbon dioxide detection consists of a carbon dioxide discharge lamp to radiate a band near 4.3 μm, a quartz tube as the sample cell, and a photoconductive cell with an interference filter to isolate the carbon dioxide band at 4.3 μm. Whereas none of the gases tested interferes with the determination of carbon dioxide, halothane and nitrous oxide, and to lesser extents, water vapor and carbon dioxide, can interfere with determination of oxygen if they are present in sufficiently high concentrations. However, when room air or air enriched with oxygen is breathed, the outputs of the oxygen and carbon dioxide detectors are not subject to interference. The feasibility of using the instrument system to rapidly detect potentially fatal complications was demonstrated by monitoring the effect of halothane anaesthesia on pigs that were susceptible to malignant hyperthermia.

ACKNOWLEDGMENT

We thank personnel at Opthos Instruments for providing optical spectra for the oxygen and xenon discharge lamps.

Registry No. O_2, 7782-44-7; CO_2, 124-38-9.

REFERENCES

(1) Modell, J. H. *Minimum Requirements for Monitoring Anaesthesiology*; 1986; Vol. 64, pp 840–841.
(2) Clakins, J. M. In *Future Anaesthesia Delivery Systems*; Brown, B. R., Ed.; Contemporary Anesthesia Practice; F. A. Davis Co.: Philadelphia, 1984; Vol. 8, p 137.
(3) de las Alas, V.; Geedes, L. A.; Voorhees, W. D.; Bourland, J. D.; Schoenlein, W. E. Oxygen uptake as in early indicator of hyperthermia. *J. Clin. Monitoring* **1990**, *6* (3), 186–88.
(4) May, W. S., Jr. In *International Anaesthesiology Clinics*; Raez, Jabor, Ed.; Little, Brown, & Co.: Boston, 1986; Vol. 24, p 159.

(5) Watt, R. *Med. Instrum.* **1983**, *17*, 386.
(6) Arnoudse, P. Instrumentation for breath-by-breath determination of oxygen and carbon dioxide based on nondispersive absorption measurements. Ph.D. Thesis, Purdue University, West Lafayette, IN, 1987.
(7) Philip, J. H.; Reamer, D. B. *Med. Instrum.* **1985**, *19*, 122.
(8) Westenskow, D. R.; Smith, K. W.; Coleman, D. L.; Gregonis, D. E.; Van Wagenen, R. A. *Anaesthesiology* **1989**, *70*, 350-55.
(9) Hudson, R. D. *Rev. Geophys. Space Phys.* **1951**, *9*, 305.
(10) Wantanabe, K.; Inn, E. C. Y.; Zelikoff, M. *J. Chem. Phys.* **1953**, *21*, 1026.
(11) Inn, E. C. Y.; Watanabe, K.; Zeikoff, M. *J. Chem. Phys.* **1953**, *21*, 1648.
(12) Wantanabe, K.; Zelikoff, M. *J. Opt. Soc. Am.* **1953**, *43*, 753.
(13) Lilly, J. C. In *Medical Physics*; Glasser, O., Ed.; The Yearbook Publishers: Chicago, 1950; Vol. 2, p 845.
(14) Prugger, V. H.; Ulmer, W. *Z. Angew. Phys.* **1959**, *11*, 467.
(15) Wilkinson, G. R.; Ford, M. A.; Price, W. C. In *Molecular Spectroscopy*; Sell, George, Ed.; Institute of Petroleum: London, 1955; p 192.
(16) Mould, H. M.; Price, W. C.; Wilkinson, G. R. *Spectrochim. Acta* **1960**, *16*, 479.
(17) Cohen, D.; Lowe, R.; Hamson, J. *J. Appl. Phys.* **1957**, *28*, 737.
(18) Gleason, W. S.; Pertek, R. *Rev. Sci. Instrum.* **1971**, *42*, 1638.
(19) Sullivan, J. O.; Holland, A. C. *NASA CR-371* **1966**.
(20) Dumas, J.-M.; Dupuis, P.; Pfister-Guillouzo, Sandorfy, C. *Can. J. Spectrosc.* **1981**, *26*, 102.
(21) Ozanne, G. M.; Young, W. G.; Mazzei, W. J.; Severinghaus, J. W. *Anaesthesiology* **1981**, *55*, 62.

RECEIVED for review October 1, 1991. Accepted October 11, 1991. This work was supported in part by Grants No. GM13326-19, from the National Institutes of Health, Bethesda, MD, and HL13725, H137345, and HL33315 from the National Heart, Lung, and Blood Institute.

Labile Hydrogen Counting in Biomolecules Using Deuterated Reagents in Desorption Chemical Ionization and Fast Atom Bombardment Mass Spectrometry

Alessandro Guarini,* Gianfranco Guglielmetti, and Nunzio Andriollo

Istituto Guido Donegani, Via G. Fauser 4, 28100 Novara, Italy

Marco Vincenti

Dipartimento di Chimica Analitica, Università di Torino, Via P. Giuria 5, 10125 Torino, Italy

The number of mobile hydrogens in biomolecules can be determined by fast atom bombardment (FAB) and desorption chemical ionization (DCI) mass spectrometry in association with, respectively, condensed-phase and gas-phase H/D exchange reactions. From the difference of molecular ion masses recorded before and after D labeling, the number of mobile hydrogens could be easily determined on a variety of macrocyclic antibiotics, carrying up to 20 mobile hydrogens, as well as on some peptides and saccharides. In FAB experiments a new procedure has been developed which involves an in situ deuteration of both sample and matrix by repeated treatment with D_2O directly on the FAB probe tip. This versatile procedure achieves high levels of deuterium substitution (94%-96%), avoids the risk of H/D back-exchange with atmospheric water, and allows the use of any water-soluble FAB matrix. In the DCI method the sample is instantly evaporated in the cold ion source filled with a rather high pressure of deuterated ammonia (ND_3). Under such conditions, both molecular and fragment ions leaving the ion source have undergone an almost complete (90%-98%) H/D exchange process with ND_3. The presence of D-labeled fragment ions in DCI mass spectra significantly helps the comprehension of molecular structures and fragmentation mechanisms. Experimental parameters influencing the extent of H/D exchange are discussed in detail.

INTRODUCTION

Recent years have seen a growing involvement of industry in biotechnological research (*1*). Most effort in this field has been addressed to the isolation of new biologically active substances extracted from microbial cultures. This method has often been selected because it is the most likely to yield commercially valuable products in a reasonably short period of time and because the technologies for selecting and growing the microorganisms and for recovering the products are rather well established (*2*).

The analytical chemists play a crucial role within the biotechnological research team in that they must immediately establish the novelty of a substance as soon as it is extracted from the fermentation broth. The characterization of an unknown substance at the very early stage of production and purification is extremely difficult because only a small amount of active substance is available and it is often mixed with extraneous compounds. Thus, a combination of various spectroscopic techniques and data-base searches is required to tackle this task.

At a preliminary stage, mass spectrometry is often used to provide the molecular weight of the unknown substance and, possibly, some significant fragment ions; for example, a neutral loss identifying the presence of a glycosidic moiety within the structure is often encountered in the mass spectrometric analysis of these unknown antibiotics. This analytical information is then exploited to restrict the investigation field of the data-base searches.

Although these biologically active substances have extremely variable and complex structures, a common feature is the high number of hydrogen atoms bonded to heteroatoms. If the number of these hydrogens could be measured in a fast and easy way, an additional and useful parameter for characterizing the molecule would be available.

The present work was addressed the acquisition of a new structure-related parameter in the characterization of unknown antibiotic substances so that the specificity and con-

0003-2700/92/0364-0204$03.00/0